CALCULATION OF DEBYE TEMPERATURE FOR CRYSTALLINE STRUCTURES—A CASE STUDY ON Ti, Zr, AND Hf

Q. CHEN† and B. SUNDMAN

Department of Materials Science and Engineering, Royal Institute of Technology, S-10044 Stockholm, Sweden

Abstract—The methods to calculate the Debye temperature from elastic moduli have been reviewed. The approximation approach due to Moruzzi *et al.* was critically examined by considering experimental elastic constant data for all the cubic elements. It was found that many cubic elements are exceptions with regard to the assumed constant scaling factor for the expression of the average sound velocity in terms of the bulk modulus, and consequently the Debye temperature of a cubic element must be calculated from the knowledge of all the elastic constants of the system. On the other hand, a fairly constant scaling factor has been found to exist for the hexagonal elements. Through the study of experimental data, some empirical relationships have been observed between the high temperature entropy–Debye temperature $\theta_D(0)$ and the low temperature limit of the Debye temperature $\theta_D(-3)$. For those structures that are dynamically unstable at low temperatures, we proposed a way to obtain their $\theta_D(0)$ from the calculated isotropic bulk moduli. The methods have been applied to calculate the Debye temperatures of hcp, bcc, and fcc Ti, Zr, and Hf from their elastic moduli derived from ab initio calculations. The calculated results agree very well with the experimental data. © 2001 Acta Materialia Inc. Published by Elsevier Science Ltd. All rights reserved.

1. INTRODUCTION

Interest in the calculation of the Debye temperature has been increasing in both semi-empirical and theoretical phase diagram calculation areas since the Debye model offers a simple but very effective method to describe the phonon contribution to the Gibbs energy of crystalline phases. The Gibbs energy data currently used in CALPHAD (CALculation of PHAse Diagrams) applications are represented by simple polynomials [1] and the parameters thus derived are lacking any physical significance. This often makes the extrapolation of these data outside their temperature range questionable and the estimation of parameters for metastable phases very difficult. Therefore, it has been suggested [2] that the Gibbs energy of a crystalline phase should be constructed from its physical components, i.e., the ground state energy, the lattice vibrational contribution, the electronic excitation, and the electronic spin ordering, etc. This can be done for stable crystalline phases, yielding an essential verification of this method, but the main concern in the present work is metastable

structures because their physical properties are not experimentally accessible. Apparently, this is the area where theoretical calculations can play a major role.

Total energy calculations from first principles cannot only provide us with the ground state structure properties but are often used together with the Debye and Grüneisen models to derive thermophysical properties and phase stabilities at finite temperatures [3–5]. Ab initio alloy phase diagram calculations have also shown that the incorporation of the vibrational contribution to the Gibbs energy through the use of the Debye model can yield predictions in closer agreement with measurements [6, 7].

Theoretical calculations of the phonon density of states and thus the Debye temperature have been possible recently by using the frozen phonon approach [8], linear response theory [9], or ab initio force constant method [10, 11]. However, all these schemes are computationally very demanding. Fortunately, we don't need to know the details of the phonon spectrum in order to calculate the Debye temperature. In its original derivation [12], the Debye temperature is related to the sound velocity and can be calculated either rigorously or approximately from elastic constants [13, 14]. The elastic constants can now be obtained from first principles without too

---

† To whom all correspondence should be addressed.
E-mail address: qing@met.kth.se (Q. Chen)

much effort [15–17]. For nonmagnetic cubic systems, Moruzzi *et al*. [3] proposed a further approximation in which the Debye temperature is directly correlated to the ab initio calculated bulk modulus. This method has gained wide use because of its simplicity and the ease to obtain the bulk modulus. However, to our knowledge, this method has not been systematically validated.

The ordinary Debye temperature, as referred to above, is the low temperature limit of the Debye temperature $\theta_D(-3)$. The notation $\theta_D(-3)$ is a special case of the Debye temperatures $\theta_D(n)$ which are derived from the nth moment of the phonon frequencies [14] (see Section 3). For phase diagram and thermodynamic calculations, the Debye temperature of interest is the high temperature entropy–Debye temperature $\theta_D(0)$, another special case of $\theta_D(n)$ and related to the logarithmic average of the phonon frequencies. In an ideal Debye solid, all $\theta_D(n)$ are equal to $\theta_D(-3)$, which can be obtained from either low temperature elastic constant or heat capacity data. In a real solid, however, $\theta_D(0)$ is different from $\theta_D(-3)$. Therefore, we must have an idea how different is $\theta_D(0)$ from $\theta_D(-3)$. Besides, it has been shown that many non-equilibrium phases are dynamically unstable at low temperatures [18–20]. In this case, $\theta_D(-3)$ is not definable, but they should have a $\theta_D(0)$ if they eventually become dynamically stable at high temperatures.

In the present investigation, we first review the approximation methods for the calculation of the Debye temperature from elastic moduli and focus on a detailed examination of the approach due to Moruzzi *et al*. [3]. Then, we extend this approach to the hexagonal structure. In Section 3, we demonstrate the empirical relationship between $\theta_D(0)$ and $\theta_D(-3)$ through the consideration of experimental data. Section 4 is devoted to those phases that exhibit dynamical instability at low temperatures. For them, we suggest a way to obtain the high temperature entropy–Debye temperatures from ab initio calculated isotropic bulk moduli. In Section 5, we perform first principles total energy calculations and apply the relevant empirical relations to Ti, Zr, and Hf, and compare the calculated $\theta_D(0)$ with experimental results when possible.

2. A REVIEW OF APPROXIMATION METHODS

2.1. *Debye temperature, sound velocity, and elastic constants*

The Debye model [12–14] assumes that the solid is an elastic continuum in which all the sound waves travel at the same velocity independent of their wavelength. Thus the phonon density of state becomes parabolic and a Debye cutoff frequency, ω_D, can be determined by the normalization condition that the total number of frequencies should equal the $3N$ degrees of freedom if the solid has N atoms. The Debye temperature, θ_D, defined as a measure of the

cutoff frequency by $\theta_D = \hbar\omega_D/k_B$, is then proportional to the Debye sound velocity v_D:

$$\theta_D = \frac{\hbar}{k_B}\left(\frac{6\pi^2 N}{V}\right)^{1/3} v_D, \qquad (1)$$

where V is the volume of the solid. In a real solid, there are three different types of sound velocities and they are generally anisotropic. It can be shown that [14]

$$\frac{1}{v_D^3} = \frac{1}{3}\sum_{i=1}^{3}\int\frac{1}{v_i^3(\theta,\phi)}\frac{d\Omega}{4\pi}, \qquad (2)$$

where (θ,ϕ) are angular coordinates and $d\Omega = \sin\theta d\theta d\phi$. If the elastic constants of the crystal are known, $v_i(\theta,\phi)$ can be obtained by solving a secular equation, and v_D and θ_D can then be calculated by numerical integration over θ and ϕ [13, 14]. For an elastically isotropic medium, v_i is independent of crystallographic directions, but different for the longitudinal and the two degenerate transverse branches. In this case, equation (2) can be greatly simplified and one has [13, 14]

$$\frac{1}{v_D^3} = \frac{1}{3}\left(\frac{1}{v_L^3} + \frac{2}{v_S^3}\right), \qquad (3)$$

where v_L and v_S are longitudinal and transverse sound velocities, and they are related to the longitudinal and transverse moduli (L and S) and the density (ρ) by $v_L = \sqrt{L/\rho}$ and $v_S = \sqrt{S/\rho}$. With the above equation, a much simpler method has been suggested for the calculation of the (average) Debye sound velocity and Debye temperature. In this method [13], the bulk modulus B and Poisson ratio v of a polycrystalline material is estimated from the single crystal elastic constants by the Voigt–Reuss–Hill (VRH) approximation [21] (see Appendix A) and then used to calculate the longitudinal and transverse moduli by

$$L = \frac{3(1-v)}{1+v}B, \qquad (4)$$

$$S = \frac{3(1-2v)}{2(1+v)}B. \qquad (5)$$

Therefore, one obtains

$$v_D = k(v)\sqrt{\frac{B}{\rho}}, \qquad (6)$$

$$\theta_D = k(v)\frac{\hbar}{k_B}\left(\frac{6\pi^2\rho}{M}\right)^{1/3}\sqrt{\frac{B}{\rho}}, \qquad (7)$$

where

$$k(v) = \left[\frac{1}{3}\left[\left[\frac{1+v}{3(1-v)}\right]^{3/2}\right.\right.$$
$$\left.\left. + 2\left[\frac{2(1+v)}{3(1-2v)}\right]^{3/2}\right]\right]^{-1/3}, \tag{8}$$

and M is the atomic weight. Anderson [13] has shown that this method gives a value for the Debye sound velocity very close to that obtained by the rigorous method after equation (2). Hence the Debye temperature can be very accurately calculated from the experimental data on elastic constants and density using equation (7), which can be rewritten as

$$\theta_D = k(v)\frac{\hbar}{k_B}(48\pi^5)^{1/6}\sqrt{\frac{r_0 B}{M}} \tag{9}$$

for the convenience of theoretic calculations. In this expression, r_0 is the equilibrium Wigner–Seitz radius, which is defined by $4\pi r_0^3/3 = V/N = M/\rho$.

2.2. Correlation between the Debye temperature and bulk modulus

As shown above, the Debye sound velocity or temperature can be calculated either rigorously or approximately from the knowledge of elastic constants. However, in a first principles calculation, computing all of these quantities is not easy compared to deriving bulk moduli from the calculated binding curves. Therefore, a further approximation would be helpful. By examining Anderson's data [13], Moruzzi et al. [3] found empirical relations between the longitudinal and shear modulus and the bulk modulus for nonmagnetic cubic elements: $L = 1.42B$ and $S = 0.30B$, which correspond to $v \approx 0.364$ in equations (4) and (5). As a result, $k(v)$ in equations (6) and (7) becomes a constant and they obtained $k^{NM-Cub} = k(0.364) = 0.617$. In this approach, the Debye sound velocity and Debye temperature are then directly expressed in terms of the bulk modulus through the use of the so-called scaling factor [3] k^{NM-Cub}. Because of its simplicity, this approach has now been used in many theoretical investigations to derive thermophysical properties at finite temperatures for pure elements and ordered compounds [3–7]. However, it seems that this method has not been systematically investigated. In their original work, Moruzzi et al. [3] selected data for only 10 nonmagnetic bcc or fcc metals to demonstrate the validity of this simplification. We shall now make a thorough examination of the universality of the scaling constant k^{NM-Cub} and also check if there is a scaling constant k^{Hcp} for the hcp structure.

2.2.1. Cubic systems.
The elastic constant data for 34 cubic elements were mainly taken from the Landolt–Börnstein handbook [22, 23], and then used to calculate the bulk modulus (B) and Poisson ratio (v) for each element with the VRH approximation method [21]. After that, the longitudinal and transverse moduli are calculated according to equations (4) and (5). The calculated results are listed in Table 1 and plotted in Figs 1–3. The 10 elements selected by Moruzzi et al. [3] are marked with filled symbols in Figs 1–3, and it is seen that all of them (except for Mo) are indeed falling on or close to the dashed line corresponding to $v = 0.364$. However, it is interesting to note that most of the data not used by them are more or less far away from the "universal" line, especially for the shear modulus data in Fig. 2. This is understandable because shear modulus is more sensitive to the variation of the Poisson ratio v. As a matter of fact, we can easily see from Fig. 3 that the v values vary systematically across the periodic table in the range from 0.2 to about 0.4 except for the extreme cases of C, Au, and Pb. As a result, $k(v)$ will change from 0.954 to 0.524 (see Fig. 4) or, in other words, from $1.550k^{NM-Cub}$ to $0.849k^{NM-Cub}$, which means that using the scaling constant $k^{NM-Cub} = 0.617$ could possibly underestimate the Debye temperature by 35% or overestimate it by 18%. It is clear from Fig. 3 that the scaling constant k^{NM-Cub} is adequate only for those elements close to the maxima, not for the other elements. Therefore, we conclude that there is no universal scaling constant for all the cubic systems, nor for the nonmagnetic cubic systems. Instead, the Debye temperature of a cubic system must be calculated from the knowledge of all the elastic constants of the system. If for any reason one has to estimate the Debye temperature from the bulk modulus alone, large uncertainties should be attached to the results.

We shall now develop an explanation for the systematic change of the Poisson ratio values shown in Fig. 3 according to the theoretic work by Fast et al. [16] and Wills et al. [18]. For convenience, we use the Voigt approximation [21] (see Appendix A). According to equation (A3), the Poisson ratio is dependent on the so-called normalized shear constant S/B [18], which in turn is determined, from equation (A2), by C'/B and C_{44}/B, where C' is the tetragonal shear constant and it equals $(C_{11}-C_{12})/2$. It is evident from equation (A3) that the larger the normalized shear constant, the smaller the Poisson ratio. The experimental and theoretical data for the normalized elastic constants are shown in Fig. 5. Note that S/B is around 0.6 for the elements close to the maxima but not for the others, and C'/B and C_{44}/B are near 0.6 only for the transition metals close to the maximum. When the Cauchy relation, $C_{12}=C_{44}$, is valid, one obtains $S/B = 0.6$ from equations (A1) and (A2). If the cubic lattice is also isotropic, i.e., $C_{44} = (C_{11}-C_{12})/2$, one has $C'/B = C_{44}/B = 0.6$. Figure 5(c) suggests that the Cauchy relation is well satisfied by the elements close to the maxima but not so well

Table 1. The elastic constants and VRH elastic moduli for cubic elements[a]

Element	C_{11} (Mbar)	C_{12} (Mbar)	C_{44} (Mbar)	B (Mbar)	L (Mbar)	S (Mbar)	v
Li	0.139	0.117	0.099	0.124	0.183	0.044	0.346
Na	0.076	0.063	0.043	0.067	0.095	0.021	0.361
K	0.037	0.032	0.019	0.034	0.045	0.009	0.381
Rb	0.033	0.027	0.020	0.029	0.042	0.010	0.352
Cs	0.025	0.015	0.021	0.018	0.034	0.012	0.235
Ca[b]	0.250	0.150	0.200	0.183	0.337	0.115	0.241
Sr[c]	0.156	0.102	0.121	0.120	0.209	0.067	0.267
Ba[d]	0.130	0.076	0.118	0.094	0.182	0.066	0.218
La[e]	0.345	0.204	0.180	0.251	0.416	0.124	0.289
Ti[f]	1.280	0.970	0.470	1.073	1.476	0.302	0.372
Hf[e]	1.340	0.960	0.659	1.087	1.622	0.401	0.336
V	2.300	1.200	0.432	1.567	2.201	0.476	0.362
Nb	2.450	1.320	0.284	1.697	2.197	0.375	0.397
Ta	2.620	1.560	0.826	1.913	2.835	0.691	0.339
Cr	3.460	0.660	1.000	1.593	3.119	1.145	0.210
Mo	4.590	1.680	1.110	2.650	4.300	1.237	0.298
W	5.170	2.030	1.570	3.077	5.170	1.570	0.282
Re[e]	5.620	2.660	2.619	3.647	6.424	2.083	0.260
Fe	2.300	1.350	1.170	1.667	2.753	0.815	0.290
Os[e]	6.610	2.970	3.323	4.183	7.663	2.610	0.242
Co	2.600	1.600	1.100	1.933	3.002	0.802	0.318
Rh	4.130	1.940	1.840	2.670	4.662	1.494	0.264
Ir	5.800	2.420	2.560	3.547	6.437	2.167	0.246
Ni	2.470	1.530	1.220	1.843	2.953	0.832	0.304
Pd	2.240	1.730	0.716	1.900	2.531	0.474	0.385
Pt	3.470	2.510	0.765	2.830	3.676	0.635	0.396
Cu	1.690	1.220	0.753	1.377	2.007	0.473	0.346
Ag	1.230	0.920	0.453	1.023	1.417	0.295	0.369
Au	1.900	1.610	0.423	1.707	2.074	0.276	0.423
Al	1.080	0.620	0.283	0.773	1.121	0.260	0.349
C	10.400	1.700	5.500	4.600	11.276	5.007	0.101
Si	1.650	0.640	0.792	0.977	1.858	0.661	0.224
Ge	1.290	0.480	0.671	0.750	1.481	0.548	0.206
Pb	0.488	0.414	0.148	0.439	0.553	0.085	0.409

[a] Elastic constant data are from [22,23] except for Ca, Sr, Ba, La, Ti, Hf, Re, and Os.
[b] From [24]. The data given in [22, 23] for Ca and Sr yeild a larger bulk modulus for Ca than that for Sr. This is believed to be wrong according the trend in IA group and the data for Be and Mg in Table 2. Also, there is no data for Ba in either Ref. 22 or Ref. 23. Recent work [24, 25] were found for the three elements and the experimental results give most probably correct order on the calculated bulk moduli.
[c] From [25].
[d] From [25].
[e] For fcc structure, calculated from theoretical data on $C'(C'=(C_{11}-C_{12})/2)$, C_{44}, and $B(B=(C_{11}+2C_{12})/3)$ reported in [18].
[f] For fcc structure, ab initio calculated in this work, see Section 5.

Table 2. The elastic constants and VRH elastic moduli for hexagonal elements[a]

Element	C_{11} (Mbar)	C_{12} (Mbar)	C_{13} (Mbar)	C_{33} (Mbar)	C_{44} (Mbar)	B (Mbar)	L (Mbar)	S (Mbar)	v
Be	2.920	0.240	0.060	3.490	1.630	1.115	3.129	1.510	0.033
Mg	0.593	0.257	0.214	0.615	0.164	0.352	0.583	0.173	0.289
Sc	0.993	0.397	0.294	1.070	0.277	0.558	0.966	0.306	0.268
Y	0.790	0.291	0.284	0.787	0.246	0.454	0.786	0.249	0.268
Ti	1.600	0.900	0.660	1.810	0.465	1.050	1.629	0.434	0.318
Zr	1.440	0.740	0.670	1.660	0.334	0.966	1.452	0.365	0.332
Hf	1.810	0.770	0.660	1.970	0.557	1.085	1.830	0.558	0.280
Tc[b]	6.117	2.187	2.075	6.450	1.966	3.484	6.152	2.001	0.259
Re	6.160	2.730	2.060	6.830	1.610	3.650	6.033	1.788	0.289
Ru	5.630	1.880	1.680	6.240	1.810	3.107	5.655	1.911	0.245
Os[b]	8.945	2.492	2.456	10.164	1.622	4.755	8.103	2.511	0.276
Co	2.950	1.590	1.110	3.350	0.710	1.874	2.898	0.768	0.320
Cd	1.160	0.420	0.410	0.509	0.196	0.539	0.855	0.237	0.308
Zn	1.650	0.311	0.500	0.618	0.396	0.661	1.207	0.410	0.244
Tl	0.419	0.366	0.299	0.549	0.072	0.368	0.439	0.053	0.431
Pr	0.494	0.230	0.143	0.574	0.136	0.288	0.485	0.148	0.281
Nd	0.548	0.246	0.166	0.609	0.150	0.318	0.536	0.163	0.281
Gd	0.678	0.256	0.207	0.712	0.208	0.379	0.669	0.218	0.259
Tb	0.692	0.250	0.218	0.744	0.218	0.389	0.692	0.227	0.256
Dy	0.740	0.255	0.218	0.786	0.243	0.405	0.739	0.250	0.244
Ho	0.765	0.256	0.210	0.796	0.259	0.409	0.761	0.264	0.234
Er	0.841	0.294	0.226	0.847	0.274	0.447	0.823	0.283	0.239
Lu	0.862	0.320	0.280	0.809	0.268	0.476	0.838	0.272	0.261

[a] Elastic constant data are from [22, 23].
[b] From theoretical calculations reported in [16].

(a)

(a)

(b)

(b)
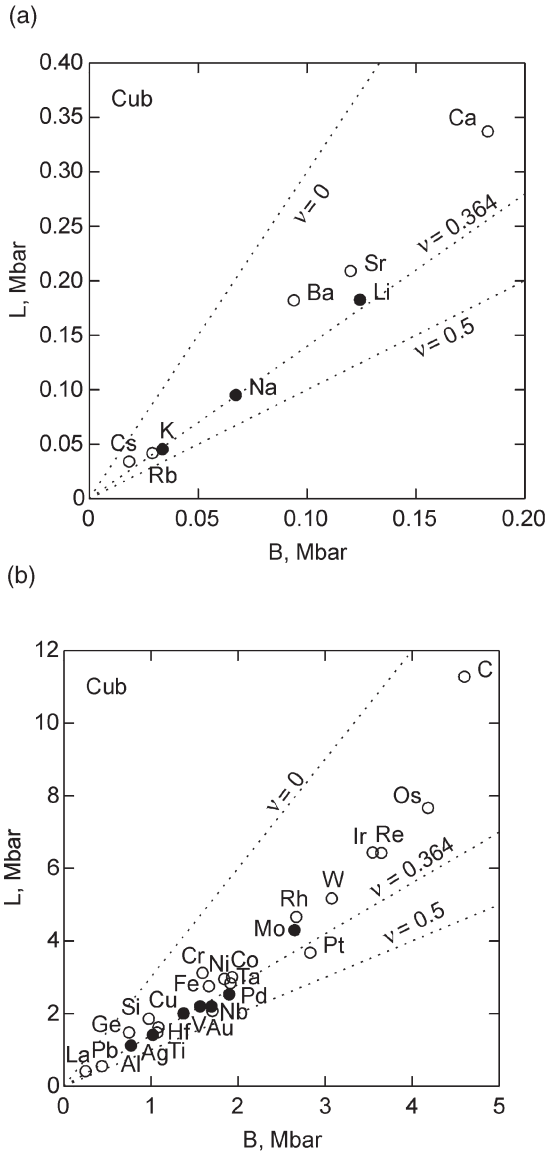
Fig. 1. The calculated isotropic longitudinal modulus (L) versus bulk modulus (B) for cubic elements in groups I–IIA (a) and the rest (b). The filled circles are for those elements selected by Moruzzi et al. [3] for illustrating the empirical relation between L and B.
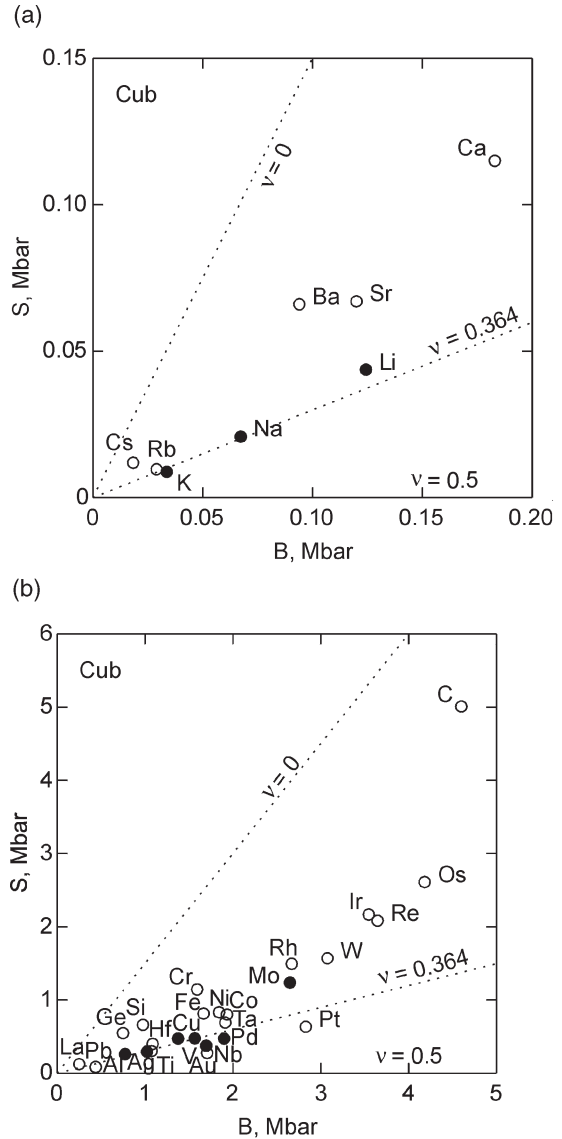
Fig. 2. The calculated isotropic shear modulus (S) versus bulk modulus (B) for cubic elements in groups I–IIA (a) and the rest (b). The filled circles are for those elements selected by Moruzzi et al. [3] for illustrating the empirical relation between S and B.

by the others. Figure 5(a) and (b) imply that the transition metals close to the maximum are also nearly isotropic. This is due to the fact that these transition metals, being bcc or fcc, are extremely stable against all kinds of shear deformation, which in turn is determined by band filling [16].

2.2.2. Hexagonal systems. Similarly, the elastic constant data for hexagonal systems were collected and processed. The results are available in Table 2 and Figs 6–8. Excluding the extreme cases of Be and Tl, the Poisson ratio values for the hexagonal systems vary only in a relatively small range from about 0.225 to 0.325 and have an average value of 0.275. According to equation (8), one gets $k^{Hex} = 0.810 \pm 0.1$.

The elastic behavior of the hexagonal system is in sharp contrast to that of the cubic systems. In their theoretical study of elastic constants of hexagonal transition metals, Fast et al. [18] demonstrated that the hexagonal transition metals obey the Cauchy relations much better than the cubic ones. This has been shown to be due to the fact that the shape of the density of states for the hexagonal materials retains its form to a larger extent, for all types of shears, than it does for many of the cubic metals. As we discussed before, the Poisson ratio increases with the decreasing of normalized shear constant S/B (see equation (A2)). Again, here we use the Voigt approximation to analyze the data. For hexagonal systems, according to
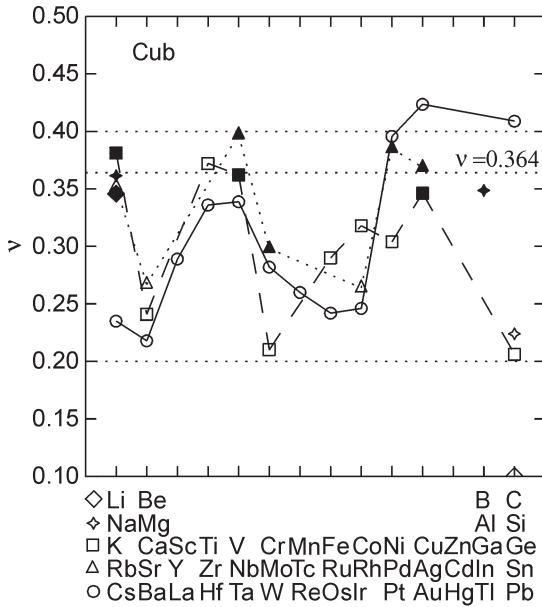
Fig. 3. The calculated Poisson ratio for cubic elements. The filled symbols are for those elements selected by Moruzzi *et al.* [3] for illustrating the empirical relations between *L*, *S*, and *B*, i.e., $\nu=0.364$.
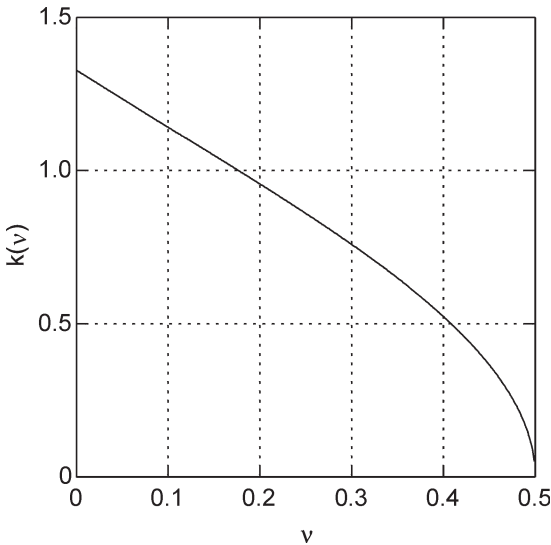
Fig. 4. The variation of $k(\nu)$ with the Poisson ratio ν.

Fig. 5. The normalized shear elastic constants for cubic elements. The filled symbols are for those elements selected by Moruzzi *et al.* [3] for illustrating the empirical relations between *L*, *S*, and *B*.

equation (A8), S/B is determined by C_{66}/B, C_{44}/B, and $(C_{11}+C_{12}+2C_{33}-4C_{13})/B$. In this case, if the Cauchy relation holds, i.e., $C_{13}=C_{44}$ and $C_{12}=C_{66}=(C_{11}-C_{12})/2$, we have $S/B=0.6$; if the system is also isotropic, i.e., $C_{11}=C_{33}$ and $C_{12}=C_{13}=C_{44}$, we have $C_{66}/B=C_{44}/B=0.6$ and $(C_{11}+C_{12}+2C_{33}-4C_{13})/B=3.6$. The available experimental and theoretical data for all the normalized elastic constants are shown in Fig. 9(a) to (d). As can be easily seen, the values of C_{66}/B, C_{44}/B and S/B are scattered around 0.6 and that of $(C_{11}+C_{12}+2C_{33}-4C_{13})/B$ around 3.6 for all the

metals except for Be and Tl. This confirms Fast *et al.*'s suggestion [18] that the hexagonal metals satisfy the Cauchy relation very well and they are quite isotropic.

3. THE RELATIONSHIP BETWEEN $\theta_D(-3)$ AND $\theta_D(0)$

Since the Debye model considers the solid as an elastic continuum, it is only satisfactory in the limit of
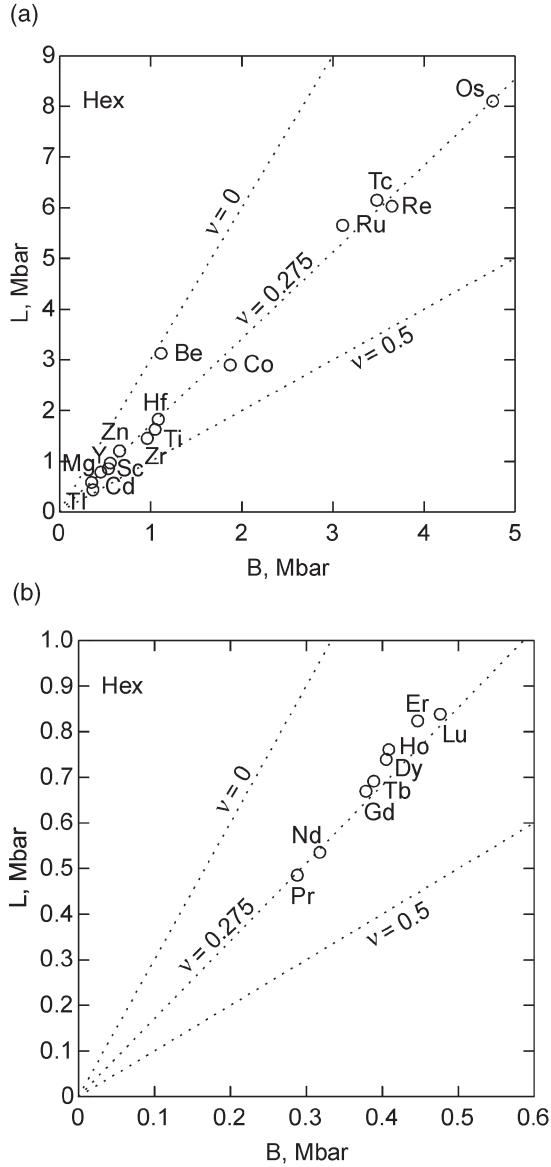
(a)

(a)

(b)

(b)

Fig. 6. The calculated isotropic longitudinal modulus (L) versus bulk modulus (B) for hexagonal non-rare-earth elements (a) and rare earth elements (b).

Fig. 7. The calculated isotropic shear modulus (S) versus bulk modulus (B) for hexagonal non-rare-earth elements (a) and rare earth elements (b).

long wavelengths or low temperatures, and the Debye temperature θ_D derived from the elastic moduli corresponds only to the low temperature limit of the Debye temperature, i.e., the Debye temperature derived from heat capacity data at very low temperatures where the T^3 law holds. In real solids, due to phonon dispersions and anharmonicity, the actual phone density of state, $F(\omega)$, are usually much more complicated than being parabolic, but it is still very useful to use the Debye spectrum to define Debye temperatures $\theta_D(n)$ $= \hbar\omega_D(n)/k_B$ so that the nth moment calculated from $F(\omega)$, normalized to 3 per atom, is equal to the nth
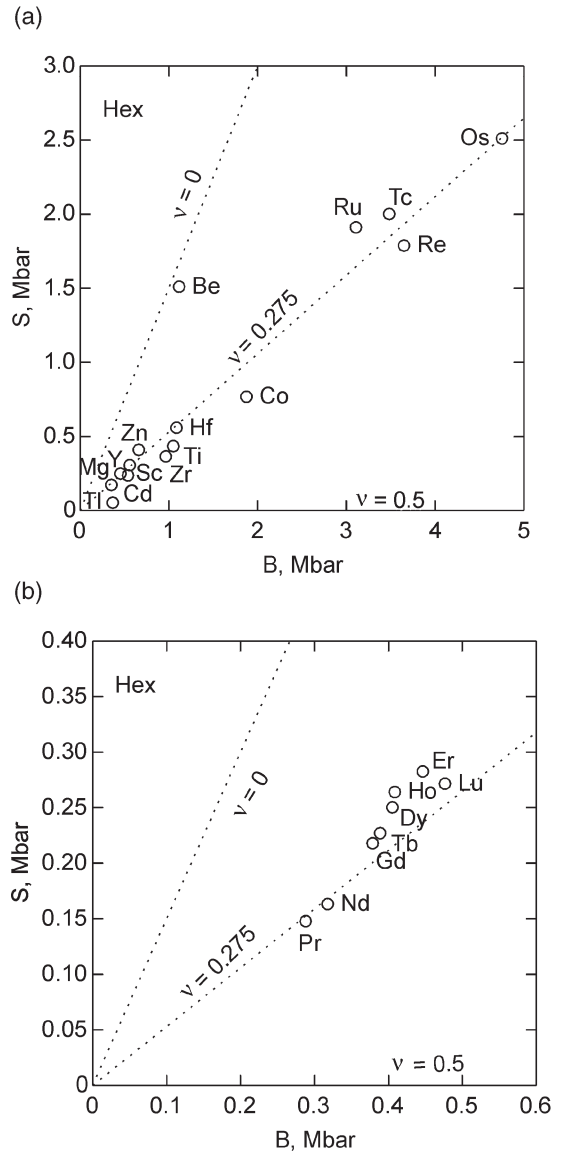
moment calculated from a Debye spectrum with the cutoff frequency $\omega_D(n)$:

$$\frac{\int_0^{\omega_D(n)} \omega^n \omega^2 d\omega}{\int_0^{\omega_D(n)} \omega^2 d\omega} = \frac{\int_0^{\omega_{max}} \omega^n F(\omega) d\omega}{\int_0^{\omega_{max}} F(\omega) d\omega} \qquad (10)$$
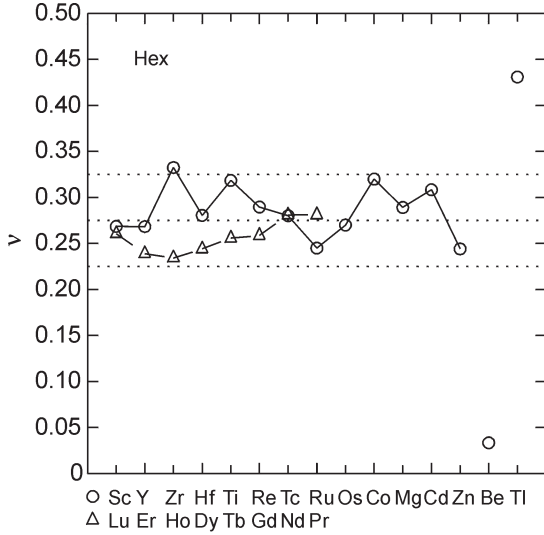
$$(n > -3, n \neq 0).$$

Fig. 8. The calculated Poisson ratio for hexagonal elements.

For $n = 0$, ω^n is replaced by $\ln(\omega)$, and thus we have

$$\omega_D(n) = \left[\frac{1}{9}(n \right. \tag{11}$$

$$\left. + 3) \int_0^{\omega_{max}} \omega^n F(\omega)d\omega \right]^{1/n} \quad (n > -3, n \neq 0),$$

$$\ln[\omega_D(0)] = \frac{1}{3}[1 + \int_0^{\omega_{max}} \ln(\omega)F(\omega)d\omega]. \tag{12}$$

Obviously, when the frequency spectrum is of the Debye type, all $\theta_D(n)$ become equal and are the same as θ_D. Also, in the limit $n = -3$, let the integrals on the both sides of equation (10) have the same diverging behavior, it can be readily shown that $\theta_D(-3)$ equals the ordinary Debye temperature θ_D [14]. The definition of $\theta_D(n)$ is particularly useful in the theory of harmonic lattice dynamics, where various thermodynamic properties can be expressed as power series containing $\theta_D(n)$. For example, the vibrational entropy has the following high-temperature expansion form:

$$S(T) = Nk_B \int_0^{\omega_{max}} \left[1 + \ln\left(\frac{k_B T}{\hbar\omega}\right) + \frac{1}{24}\left(\frac{\hbar\omega}{k_B T}\right)^2 \right.$$

$$\left. - \frac{1}{960}\left(\frac{\hbar\omega}{k_B T}\right)^4 + \ldots \right] F(\omega)d\omega = 3Nk_B \left[\frac{4}{3} \right. \tag{13}$$

$$+ \ln\left(\frac{T}{\theta_D(0)}\right) + \frac{1}{40}\left(\frac{\theta_D(2)}{T}\right)^2$$

$$\left. - \frac{1}{2240}\left(\frac{\theta_D(4)}{T}\right)^4 + \ldots \right].$$
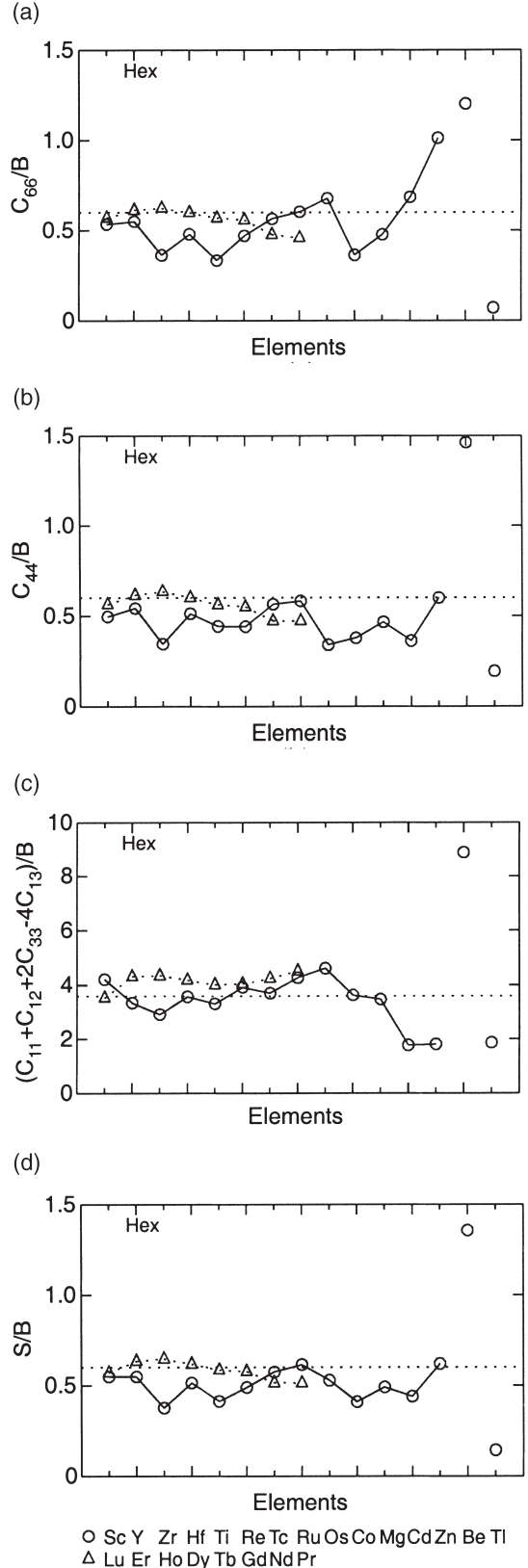
Fig. 9. The normalized shear elastic constants for hexagonal elements.

If we let the above equation equal the expression for an ideal Debye spectrum with energy cutoff frequency $k_B\theta_D^S/\hbar$, a temperature-dependent "entropy–Debye temperature" $\theta_D^S(T)$ can be defined:

$$S(T) = 3Nk_B\left[\frac{4}{3} + \ln\left(\frac{T}{\theta_D^S(T)}\right)\right.$$
$$\left. + \frac{1}{40}\left(\frac{\theta_D^S(T)}{T}\right)^2 - \frac{1}{2240}\left(\frac{\theta_D^S(T)}{T}\right)^4 + \dots\right]. \qquad (14)$$

Comparing equation (14) with equation (13), we know that $\theta_D(0)$ is equal to $\theta_D^S(\infty)$, usually called the high temperature entropy–Debye temperature because, for many solids, $\theta_D^S(T)$ does not change very much at temperatures above about $\theta_D(-3)/2$. As a consequence, it is conventional in harmonic lattice dynamics to denote the high temperature entropy–Debye temperature by $\theta_D(0)$ and the ordinary Debye temperature or the low temperature limit of the Debye temperature by $\theta_D(-3)$, and we shall follow this convention hereafter.

The relationship between $\theta_D(0)$ and $\theta_D(-3)$ is not definite according to theoretical analysis [26]. Nevertheless, we shall now examine the experimental data and see if any empirical relationship exists between $\theta_D(0)$ and $\theta_D(-3)$. Most of low temperature limit data are taken from Kittel [27]. The high temperature entropy–Debye temperature values are obtained by fitting to the experimental entropy data with a model taking electronic, anharmonic and magnetic contributions into account [28]. All the data are listed in Table 3 and plotted in Figs 10 and 11. From the plottings, some trends have been found.

Hexagonal systems can be well divided into two groups: the first, $\theta_D(0) = 0.86\theta_D(-3)$, for Mg, Sc, Y, La, Ti, Zr, Hf, and Co; the second, $\theta_D(0) = 0.68\theta_D(-3)$ for Tc, Re, Ru, Os, Zn, Cd, and Be. It is interesting to note that all the elements except for Co from the first group are on the left side of the periodic table while all except for Be from the second group are on the right side. We may guess that, if it were not for its extreme elastic stiffness, Be would be in the first group; and, if it were not for its electronic spin ordering, Co would be in the second group.

Cubic systems may be divided into three categories: the first, $\theta_D(0) = 1.07\theta_D(-3)$, for IA metals; the second, $\theta_D(0) = 0.94\theta_D(-3)$, for the cubic IIA, VB, VIIIBc (except for magnetic Ni), IB (except for Au), IIIA, and IVA (except for C) systems; the third, where $\theta_D(0)/\theta_D(-3)$ is in the range 0.66~0.87, for VIB–VIIIBb cubic elements (except for magnetic Fe). It is interesting to note that the last group consists of the transition elements located between the maxima in Fig. 3.

Considering the exceptions mentioned above, it seems that the relationship between $\theta_D(0)$ and $\theta_D(-3)$ is influenced somehow by the elastic behavior and magnetism. Magnetism always places metals in the "wrong" group and it does the same to the elastic

behavior (see Fig. 3). Cobalt, which should belong to the second hexagonal group as discussed above, is actually in the first group; iron, which should belong to the third cubic group, may actually be considered as one in the second cubic group; and nickel, which should belong to the second cubic group, may be assigned to the third cubic group. Super "soft" (with very large ν value) elements (Au and Tl) tend to have $\theta_D(0)/\theta_D(-3)$ values larger than unity. Super "hard" (with very small ν value) materials (Be and C) tend to have $\theta_D(0)/\theta_D(-3)$ values smaller than that of most metals. We also note that the average value of the last cubic group is about the same as the average for all the hexagonal elements (0.76). This again implies that the $\theta_D(0)/\theta_D(-3)$ ratio is related to the elasticity because, as we demonstrated in the last section, both the transition metals in the last cubic group and all the hexagonal metals exhibit nearly the same elastic behaviors, i.e., obeying the Cauchy relation very well and being almost elastically isotropic.

4. EFFECT OF DYNAMICAL INSTABILITY

First principles calculations [18–20] have shown that many of the non-equilibrium structures, which have been considered as metastable phases, are actually dynamically or mechanically unstable at 0 K. In this case, their tetragonal shear constants $C'[C' = (C_{11} - C_{12})/2]$ and sometimes even C_{44} are negative at low temperatures [20] and the phonon frequencies in some directions become imaginary. Therefore, $\theta_D(-3)$ is not definable for these phases. However, in the CALPHAD method, one still needs these structures as reference states for the Gibbs energy of alloys [31]. By assuming that these phases will eventually become dynamically, but not necessarily thermodynamically, stable at high temperatures due to the entropy effect, one may define a high temperature entropy–Debye temperature $\theta_D(0)$ for them. Generally speaking, the dynamical instability or negative shear modulus leads to a large Poisson ratio. In order for these phases to become dynamically stable, their Poisson ratios must have values less than 0.5. In Tables 1 and 2 or Figs 3 and 8, the largest existing Poisson ratios found for cubic and hexagonal structures are 0.423 for Au and 0.431 for Tl. Using the elastic data for other structures in the Landolt–Börnstein handbooks [22, 23] and the VRH formula given by Meister and Peselnick [21], we found two other unusually large Poisson ratios: 0.444 for tetragonal In and 0.420 for trigonal Hg. Judging from these data, we now make a further assumption that for these unstable structures to become dynamically stable, they must have a Poisson ratio of about 0.43, an average of the abnormally large values found so far. Finally, from Table 3 we found that for Au, Tl, In, and Hg, their $\theta_D(0)$ values are all larger than their $\theta_D(-3)$ values, and the ratio $\theta_D(0)/\theta_D(-3)$ is 1.15±0.09. Therefore, for these unstable structures, the high temperature entropy–Debye temperature may

Table 3. The low temperature limit of the Debye temperature $\theta_D(-3)$ and the high temperature entropy-Debye temperature $\theta_D(0)$[a]

Element	$\theta_D(-3)$, K	$\theta_D(0)$, K	$\theta_D(0)/\theta_D(-3)$	Element	$\theta_D(-3)$, K	$\theta_D(0)$, K	$\theta_D(0)/\theta_D(-3)$
Li	344	375	1.09	Fe	470	432	0.92
Na	158	161	1.02	Ru	600	397	0.66
K	91	96	1.05	Os	500	325	0.65
Rb	56	60	1.07	Co	445	372	0.84
Cs	38	43	1.13	Rh	480	357	0.74
Be	1440	960	0.67	Ir	420	293	0.70
Mg	400	326	0.82	Ni	450	379	0.84
Ca	230	229	1.00	Pd	274	264	0.96
Sr	147	133	0.90	Pt	240	228	0.95
Ba	110	102	0.93	Cu	343	321	0.94
Sc	360	306	0.85	Ag	225	216	0.96
Y[b]	240	205	0.85	Au	165	176	1.07
La	142	126	0.89	Zn	327	225	0.69
Ti	420	374	0.89	Cd	209	149	0.71
Zr	291	261	0.90	Hg	71.9	89	1.24
Hf	252	215	0.85	B[d]	1580	1220	0.77
V	380	359	0.94	Al	428	400	0.93
Nb	275	281	1.02	Ga	320	231	0.72
Ta	240	225	0.94	In	108	121	1.12
Cr	630	500	0.79	Tl	78.5	90	1.15
Mo	450	391	0.87	C	2230	1786	0.80
W	400	325	0.81	Si	645	584	0.91
Mn	410	369	0.90	Ge	374	338	0.90
Tc[c]	504	332	0.66	Sn	200	158	0.79
Re	430	277	0.64	Pb	105	92	0.88

[a] All the $\theta_D(-3)$ data are from [27] except for that of Y and Tc. All the $\theta_D(0)$ data are from [28].

[b] The $\theta_D(-3)$ data is from [29]. The value (280 K) given in [27] is discarded because it is much larger than the experimental data (240 K) compiled in [29] and the elastic Debye temperature (257 K) calculated in [13].

[c] No experimental $\theta_D(-3)$ data is available. The value given here is calculated from the estimated bulk modulus ([16]) and experimental volume data (quoted in [16]) using the approach due to Moruzzi et al. ([3]) with the scaling constant for hexagonal structure, k^{Hex}, found in this study.

[d] The $\theta_D(-3)$ value, not available in [27], is taken from [30].
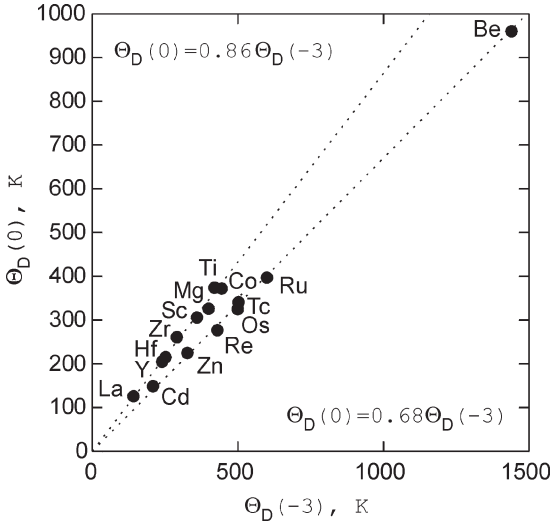
Fig. 10. The experimental $\theta_D(0)$ versus $\theta_D(-3)$ for hexagonal systems.
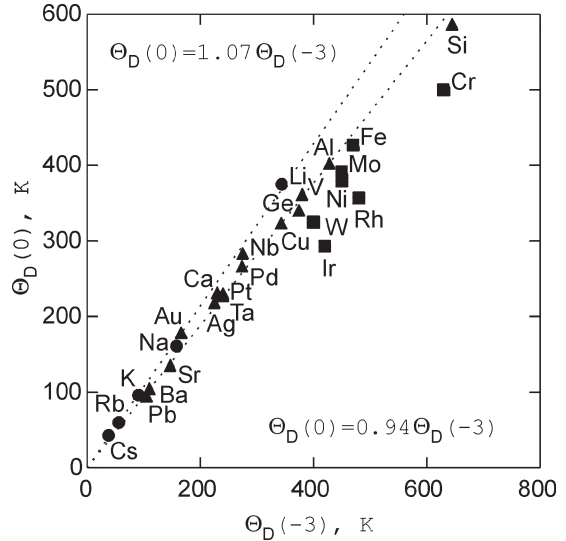
Fig. 11. The experimental $\theta_D(0)$ versus $\theta_D(-3)$ for cubic elements.

be obtained in line with Moruzzi et al.'s approach by linking it with the isotropic bulk modulus:

$$\theta_D(0) = 1.15k(0.43)\frac{\hbar}{k_B}(48\pi^5)^{1/6}\sqrt{\frac{r_0 B}{M}} \quad (15)$$

$$= 0.5\frac{\hbar}{k_B}(48\pi^5)^{1/6}\sqrt{\frac{r_0 B}{M}}.$$

5. CASE STUDY OF Ti, Zr, AND Hf

5.1. Total energy calculation

The calculations were performed by using the CAmbridge Serial Total Energy Package (CASTEP), a first principles pseudopotential plane-wave code based on the density functional theory (DFT) [32, 33] and conjugate gradients algorithm [34]. For the exchange-correlation potentials we have chosen the

(a)

(b)

(c)
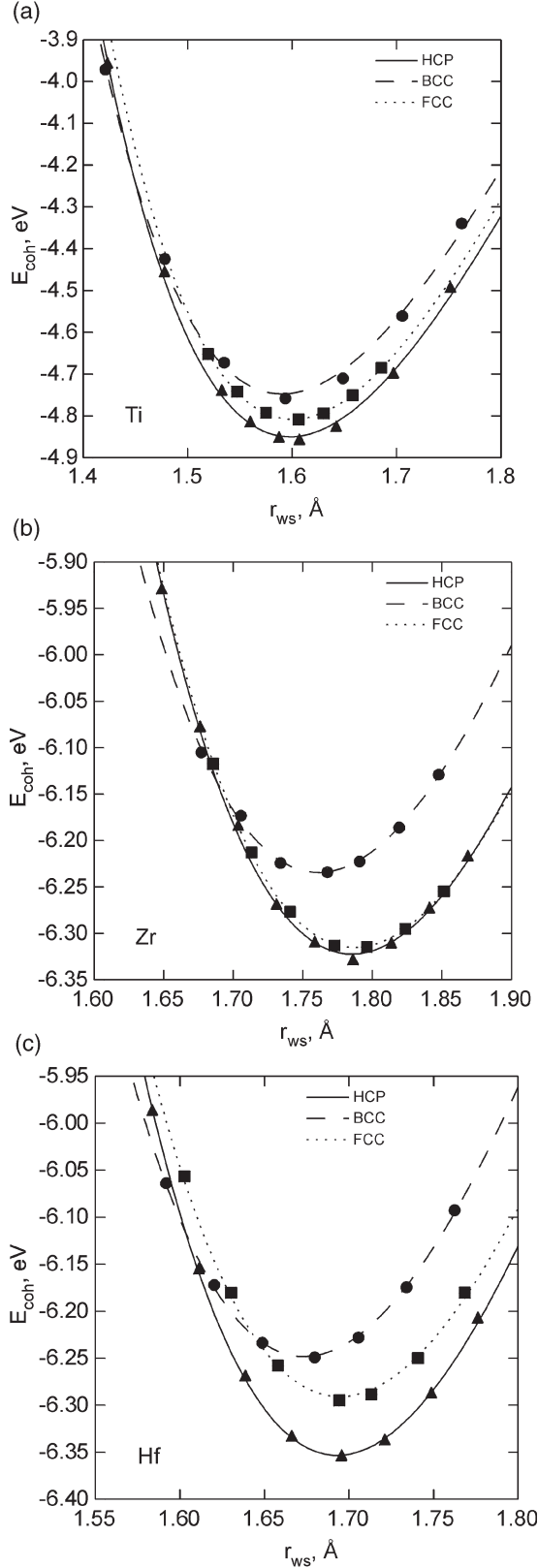
Fig. 12. The calculated binding energy for (a) Ti, (b) Zr, and (c) Hf.

local density approximation (LDA) [35] in the form as parameterized by Perdew and Wang (GGA) [36, 37]. The electron-ion interaction is described using the ultrasoft pseudopotentials generated by Lee [38] according to Vanderbilt's scheme [39]. A plane wave basis set with a 350 eV energy cutoff was used to expand the electronic wave functions for Ti, while a 270 eV cutoff was used for Zr and a 290 eV cutoff for Hf. The integration over the first Brillouin zone was approximated by sums on a regular 8×8×8 Monkhorst–Pack [40] mesh of special k-points for the bcc and fcc lattices and an 8×8×4 mesh for the hcp structure. To overcome the partial occupancy problem in metallic systems, we used a Gaussian smearing parameter of about 0.2 eV and included the entropy correction term in the total energy expression [41]. The structure properties were obtained by computing the cohesive energy at several lattice constants for different structures and then fitted to the universal equation of state for metals [42] as

$$E(r) = -|E_0|(1 + a + 0.05a^3)e^{-a}, \qquad (16)$$

where

$$a = \frac{r - r_0}{l}. \qquad (17)$$

The equilibrium energy E_0, the Wigner–Seitz radius r_0 and the length scale l are the fitting parameters, from which the bulk modulus can be obtained by [42]

$$B = \frac{|E_0|}{12\pi r_0 l^2}. \qquad (18)$$

The advantage of the use of the universal equation of state is that the derivative of the bulk modulus with pressure and the Grüneisen constant can be calculated at the same time [42]. These parameters are important for the calculation of other contributions to the Gibbs energy and estimation of thermal volume expansion of the system.

The calculated binding curves for Ti, Zr, and Hf are shown in Fig. 12. All of them correctly give hcp as the most stable structure. We also notice that the curves for the hcp and bcc phases intersect at a radius smaller than that at the minima, i.e. the equilibrium radii, which suggests that the bcc phase for all these elements will become stable at high pressures. This is in agreement with experimental findings [43, 44] and other theoretical calculations [45]. The obtained equilibrium radii and bulk moduli are listed in Table 4. The agreement between the present calculation and full-potential calculations [4, 46, 47] as well as the experimental data [27, 29, 48] is good.

Table 4. The calculated and experimental structural properties of Ti, Zr, and Hf

Element	Structure	Method	r_0(Å)	B (Mbar)	$\theta_D(0)$(K)
Ti	Hcp	This work	1.598	1.053	385
		FP-LMTO [4]	1.625	1.076	
		FP-LMTO [46]	1.597	1.08	
		FP-LAPW [47]	1.57	1.25	
		PP [47]	1.561	1.33	
		Expt.	1.615 [27,48]	1.050 [27,29]	374 [28]
	Bcc	This work	1.590	1.007	269
		Expt.		1.180 [49]	263 [28], 272 [49]
	Fcc	This work	1.601	1.072	312
Zr	Hcp	This work	1.785	0.794	256
		FP-LMTO [4]	1.791	0.884	
		FP-LMTO [46]	1.773	0.912	
		Expt.	1.771 [27,48]	0.833 [27], 0.966 [29]	261 [28]
	Bcc	This work	1.761	0.779	180
		Expt.		0.967 [50]	178 [28], 175 [50]
	Fcc	This work	1.787	0.768	177
Hf	Hcp	This work	1.693	1.220	221
		FP-LAPW [47]	1.702	1.20	
		PP [47]	1.699	1.19	
		Expt.	1.748 [27,48]	1.085 [27,29]	215 [28]
	Bcc	This work	1.673	1.176	154
		Expt.		1.123 [51]	145 [28], 145 [51]
	Fcc	This work	1.695	1.123	194

5.2. Calculation of Debye temperatures

According to our demonstration in Sections 2 and 3, the high temperature entropy–Debye temperatures of hcp Ti, Zr, and Hf can be obtained from the ab initio calculated bulk moduli and equilibrium Wigner–Seitz radii by

$$\theta_D(0) = 0.86 k^{Hex} \frac{\hbar}{k_B} (48\pi^5)^{1/6} \sqrt{\frac{r_0 B}{M}} \qquad (19)$$
$$= 0.70 \frac{\hbar}{k_B} (48\pi^5)^{1/6} \sqrt{\frac{r_0 B}{M}}.$$

The calculated results are given and compared with experimental data in Table 4 and Fig. 13. As
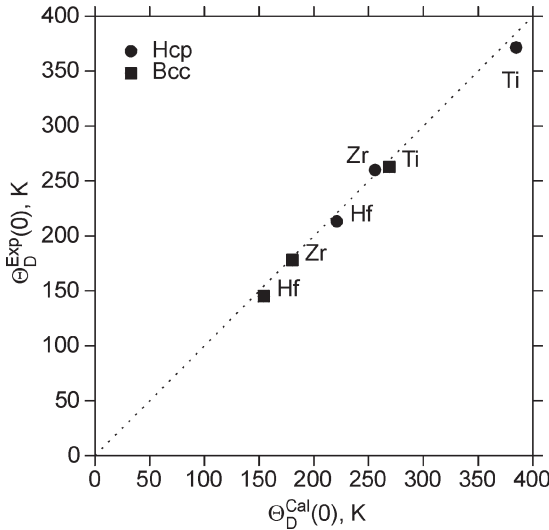
Fig. 13. Comparison of the calculated and experimental high temperature entropy–Debye temperature $\theta_D(0)$ for hcp and bcc Ti, Zr, and Hf.

expected, the agreement between the calculations and experiment is satisfactory because the theoretically calculated bulk moduli and equilibrium volumes are close to the experimental data, and the empirical relation between $\theta_D(0)$ and $\theta_D(-3)$ is obtained using the experimental data including those of Ti, Zr, and Hf. We shall now have a look at the bcc and fcc structures, which are unstable and metastable in the ground state, respectively

It is well known that bcc Ti, Zr, and Hf are dynamically unstable at the ground state and become dynamically stiff and thermodynamically stable at high temperatures [45, 47]. Thus they offer us a unique opportunity to test our assumptions made in Section 4 by comparing the calculations with experiments. The experimental Debye temperatures were obtained both from the inelastic neutron scattering measurements [49–51] and by fitting to the high temperature entropy data with a model taking care of electronic, anharmonic and magnetic contributions at the same time [28]. The experimental data are given in Table 4 and it is seen that they are close to each other. Using equation (15), we have calculated the $\theta_D(0)$ for bcc Ti, Zr, and Hf. The results are listed in Table 4. They are also shown together with the experimental data [28] in Fig. 13. To our surprise, the agreement between the calculations and experiments is remarkably good considering the speculative arguments behind the calculation method. It should be mentioned that the experimental data for bcc Ti, Zr, and Hf have not been considered during the formulation of equation (15). The success on bcc Ti, Zr, and Hf is encouraging and a similar study on bcc Sc, Y, and La has been carried out and the results turned out to be equally good [52].

Fcc Ti, Zr and Hf are not thermodynamically stable in nature, but their Gibbs energy is of interest

to the alloy phase diagram calculations [31]. Therefore, we also need to know their Debye temperatures. Considering the instability of the bcc structure against tetragonal deformation in these systems, it is clear that the corresponding fcc structure is dynamically stable. For cubic systems, as we found before, the use of the approximation method due to Moruzzi et al. [3] involves very large uncertainties. So the elastic constants of fcc Ti have been determined in this study by calculating the elastic energy density as a function of small strains applied to the equilibrium lattice [15]. The calculated results are:

$$C_{11} = 1.28, \ C_{12} =$$

0.97, and $C_{44} = 0.47$, from which the Poisson ratio is obtained using the VRH approximation [21] and it equals 0.372. This result has already been plotted in Fig. 3 together with theoretical results [16] for fcc Hf (see also Table 1). With these values for Ti and Hf and the distinct trend shown in Fig. 3, we may estimate that the Poisson ratio of fcc Zr is around 0.40. Using equation (9), their $\theta_D(-3)$ values have been calculated. Furthermore, fcc Ti, Zr and Hf most probably belong to the second group in cubic systems with regard to the relationship between $\theta_D(0)$ and $\theta_D(-3)$, so we adopted the following relation $\theta_D(0) = 0.94\theta_D(-3)$ to calculate their $\theta_D(0)$. The calculated results are given in Table 4. It is interesting to see that, contrary to our usual assumption that the fcc and hcp structures should have very similar physical properties, the high temperature entropy–Debye temperatures of fcc Ti and Zr are 20%~30% smaller than those of the hcp structures, owing to the fact that their fcc sturctures have relatively large Poisson ratio values or small shear constants. Such low Debye temperatures imply that there is a tendency for their fcc structures to become stable at high temperatures due to the entropy effect, but they remain metastable since the vibrational entropy alone is not enough. This can be seen from the fact that the corresponding bcc structures have either an even lower or about the same Debye temperature while, at the same time, each of them has a very large contribution to the Gibbs energy from electronic thermal excitations [4], which works together with the vibrational contribution and make the bcc structure to become thermodynamically stable before the solid lattice melts down.

6. SUMMARY AND CONCLUSIONS

The methods to calculate the Debye temperature from first principles results have been reviewed. The approximation method due to Moruzzi et al. [3] has been critically examined by considering both experimental and theoretical elastic constant data for all the cubic elements. It was found that many cubic elements are exceptions regarding to the assumed constant scaling factor for the expression of the average sound velocity in terms of the bulk modulus. It

was concluded that the Debye temperature of a cubic element must be calculated from the knowledge of all the elastic constants of the system. On the other hand, for the hexagonal elements we found that a fairly constant scaling factor, 0.81, can be used to calculate the Debye temperature from the bulk modulus. This difference between the cubic and hexagonal systems has been explained using the trend found for their elastic constants, which in turn is determined by the details of their density of states [16, 18]. In order to obtain the high temperature entropy–Debye temperature $\theta_D(0)$, the experimental data available for almost all the unary systems have been studied and some empirical relations between $\theta_D(0)$ and $\theta_D(-3)$ have been observed. For those structures that are dynamically unstable at low temperatures, we proposed a way to obtain their high temperature entropy–Debye temperatures from the calculated isotropic bulk moduli by using a scaling factor of 0.5. The methods have been applied to calculate the Debye temperatures for hcp, bcc, and fcc Ti, Zr, and Hf. First principles pseudopotential plane-wave calculations have been performed and the binding energy curves have been obtained. The bulk moduli for different structures were derived by using the universal equation of state for metals. The elastic constants of fcc Ti were also computed and then used to calculate the Poisson ratio for the adjustment of the scaling factor. The calculated Debye temperatures agree very well with the values derived from the high temperature experimental entropy data.

REFERENCES

1. Dinsdale, A., *Calphad*, 1991, **15**, 317.
2. Chase, M. W., Ansara, I., Dinsdale, A., Eriksson, G., Grimvall, G., Höglund, L. and Yokokawa, H., *Calphad*, 1995, **19**, 437.
3. Moruzzi, V. L., Janak, J. P. and Schwarz, K., *Phys. Rev. B*, 1988, **37**, 790.
4. Moroni, E. G., Grimvall, G. and Jarlborg, T., *Phys. Rev. Lett.*, 1996, **76**, 2758.
5. Ostanin, S. A. and Trubitsin, V. Yu., *Phys. Rev. B*, 1998, **57**, 13485.
6. Sanchez, J. M., Stark, J. P. and Moruzzi, V. L., *Phys. Rev. B*, 1991, **44**, 5411.
7. Asta, M., McCormack, R. and de Fontaine, D., *Phys. Rev. B*, 1993, **48**, 748.
8. Kunc, K. and Martin, R. M., *Phys. Rev. Lett.*, 1982, **48**, 406.
9. Baroni, S., Giannozzi, P. and Testa, A., *Phys. Rev. Lett.*, 1987, **58**, 1861.
10. Frank, W., Elsässer, C. and Fähnle, M., *Phys. Rev. Lett.*, 1995, **74**, 1791.
11. Kresse, G., Furthmuller, J. and Hafner, J., *Europhys. Lett.*, 1995, **32**, 729.
12. Debye, P., *Ann. d. Physik*, 1912, **39**, 789.
13. Anderson, O. L., in *Physical Acoustics, Vol. III—Part B*, ed. W. P. Mason. Academic Press, New York, 1965.

14. Grimvall, G., *Thermophysical Properties of Materials*. North-Holland, Amsterdam, 1986.
15. Söderlind, P., Eriksson, O., Wills, J. M. and Boring, A. M., *Phys. Rev. B*, 1993, **48**, 5844.
16. Fast, L., Wills, J. M., Johansson, B. and Eriksson, O., *Phys. Rev. B*, 1995, **51**, 17431.
17. Steubke-Neumann, G., Stixrude, L. and Cohen, R. E., *Phys. Rev. B*, 1999, **60**, 791.
18. Wills, J. M., Eriksson, O., Söderlind, P. and Boring, A. M., *Phys. Rev. Lett.*, 1992, **68**, 2802.
19. Craievich, P. J., Weinert, M., Sanchez, J. M. and Watson, R. E., *Phys. Rev. Lett.*, 1994, **72**, 3076.
20. Einarsdotter, K., Sadigh, B., Grimvall, G. and Ozolins, V., *Phys. Rev. Lett.*, 1994, **79**, 2073.
21. Meister, R. and Peselnick, L., *J. Appl. Phys.*, 1966, **37**, 4121.
22. Hearmon, R. F. S., in *Landolt–Börnstein Numerical Data and Functional Relationships in Science and Technology New Series, III/11*, ed. K. -H. Hellwege and A. M. Hellwege. Springer, Berlin, 1979.
23. Hearmon, R. F. S., in *Landolt–Börnstein Numerical Data and Functional Relationships in Science and Technology New Series, III/18*, ed. K. -H. Hellwege and A. M. Hellwege. Springer, Berlin, 1984.
24. Buchenau, U., Schober, H. R. and Wagner, R., *J. Phys. (Paris) Colloq.*, 1981, **42**, C6–395.
25. Buchenau, U., Heiroth, M., Schober, H. R., Evers, J. and Oehlinger, G., *Phys. Rev. B*, 1984, **30**, 3502.
26. Blackman, M., in *Handbuch der Physik*, ed. S. Flugge, Vol. VII. Springer, Berlin, 1955.
27. Kittel, C., *Introduction to Solid State Physics*, 7th ed. John Wiley and Sons, Inc, New York, 1996.
28. Chen, Q. and Sundman, B., unpublished, 2000.
29. Schober, H. R. and Dederichs, P. H., in *Landolt–Börnstein Numerical Data and Functional Relationships in Science and Technology New Series, III/13a*, ed. K. -H. Hellwege and J. L. Olsen. Springer, Berlin, 1981.
30. Tsagareusgvili, G. V., *J. Less-Common Metals*, 1980, **75**, 141.
31. Kaufman, L. and Bernstein, H., *Computer Calculation of Phase Diagrams*. Academic Press, New York, 1970.
32. Hohenberg, P. and Kohn, W., *Phys. Rev.*, 1964, **136**, B864.
33. Kohn, W. and Sham, L. J., *Phys. Rev.*, 1965, **140**, A1133.
34. Payne, M. C., Teter, M. P., Allan, D. C., Arias, T. A. and Joannopoulos, J. D., *Rev. Mod. Phys.*, 1992, **64**, 1045.
35. Perdew, J. P. and Zunger, A., *Phys. Rev., B*, 1981, **23**, 5048.
36. Perdew, J. P. and Wang, Y., *Phys. Rev., B*, 1992, **46**, 6671.
37. White, J. A. and Bird, D. M., *Phys. Rev. B*, 1994, **50**, 4954.
38. Lee, M. H., in *Cerius² software package*. MSI, San Diego, 1998.
39. Vanderbilt, D., *Phys. Rev. B*, 1990, **41**, 7892.
40. Monkhorst, H. J. and Pack, J. D., *Phys. Rev. B*, 1976, **13**, 5188.
41. Elsässer, C., Fähnle, M., Chan, C. T. and Ho, K. M., *Phys. Rev. B*, 1994, **49**, 13975.
42. Rose, J. H., Smith, J. R., Guinea, F. and Ferrante, J., *Phys. Rev. B*, 1984, **29**, 2963.
43. Xia, H., Parthasarathy, G., Luo, H., Vohra, Y. K. and Ruoff, A. L., *Phys. Rev. B*, 1990, **42**, 6736.
44. Xia, H., Duclos, S. J., Ruoff, A. L. and Vohra, Y. K., *Phys. Rev. Lett.*, 1990, **64**, 204.
45. Ahuja, R., Wills, J. M., Johansson, B. and Eriksson, O., *Phys. Rev. B*, 1993, **48**, 16269.
46. Ozolins, V. and Körling, M., *Phys. Rev. B*, 1993, **48**, 18304.
47. Persson, K., Ekman, M. and Ozolins, V., submitted to *Phys. Rev. Lett.*, 1999.
48. *American Institute of Physics Handbook*, McGraw-Hill, New York, 1970.
49. Petry, W., Heiming, A., Trampenau, J., Alba, M., Herzig, C., Schober, H. R. and Vogl, G., *Phys. Rev. B*, 1991, **43**, 10933.
50. Heiming, A., Petry, W., Trampenau, J., Alba, M., Herzig, C., Schober, H. R. and Vogl, G., *Phys. Rev. B*, 1991, **43**, 10948.
51. Trampenau, J., Heiming, A., Petry, W., Alba, M., Herzig, C., Miekeley, W. and Schober, H. R., *Phys. Rev. B*, 1991, **43**, 10963.
52. Chen, Q. and Sundman, B., unpublished, 2000.
53. Voigt, W., *Lehrbuch de Kristallphysik*, Terubner, Leipzig, 1928.
54. Reuss, A., *Z. Angew. Math. Mech.*, 1929, **9**, 49.
55. Hill, R., *Proc. Phys. Soc. London A*, 1952, **65**, 349.
56. Chung, D. H., *Philos. Mag.*, 1963, **8**, 833.

APPENDIX A

The Voigt–Reuss–Hill Approximation [14, 21]

The effective elastic moduli of polycrystalline aggregates are usually calculated by the two approximations due to Voigt [53] and Reuss [54], where uniform strain and stress are assumed throughout a polycrystal, respectively. Hill [55] has shown that the Voigt and Reuss averages are limits and suggested that the actual effective moduli could be approximated by the arithmetic mean of the two bounds, referred to as the Voigt–Reuss–Hill (VRH) value by Chung [56].

The cubic systems are characterized by three independent elastic constants C_{11}, C_{12}, and C_{44}. The Voigt bounds are

$$B_V = \frac{1}{3}(C_{11} + 2C_{12}) \qquad (A1)$$

$$S_V = \frac{1}{5}(C_{11} - C_{12} + 3C_{44}) \qquad (A2)$$

$$v_V = \frac{3B_V - 2S_V}{2(3B_V + S_V)} \qquad (A3)$$

and the Reuss bounds are

$$B_R = \frac{1}{3}(C_{11} + 2C_{12}) \qquad (A4)$$

$$S_R = \frac{5(C_{11} - C_{12})C_{44}}{4C_{44} + 3(C_{11} - C_{12})} \qquad (A5)$$

$$v_R = \frac{3B_R - 2S_R}{2(3B_R + S_R)} \qquad (A6)$$

The hexagonal system has five independent elastic constants C_{11}, C_{12}, C_{13}, C_{33} and C_{44}. The Poisson ratio bounds can be calculated according to equations (A3) and (A6) after the bulk and shear moduli are obtained by

$$B_V = \frac{1}{9}(2(C_{11} + C_{12}) + C_{33} + 4C_{13}) \quad \text{(A7)}$$

$$S_V = \frac{1}{30}(12C_{66} + 12C_{44} + M) \quad \text{(A8)}$$

where

$$M = C_{11} + C_{12} + 2C_{33} - 4C_{13} \quad \text{(A9)}$$

$$C_{66} = \frac{1}{2}(C_{11} - C_{12}) \quad \text{(A10)}$$

and

$$B_R = C^2/M \quad \text{(A11)}$$

$$S_R = \frac{5}{2}\left[\frac{C^2 C_{44} C_{66}}{3B_V C_{44} C_{66} + C^2(C_{44} + C_{66})}\right] \quad \text{(A12)}$$

where

$$C^2 = (C_{11} + C_{12})C_{33} - 2C_{13}^2 \quad \text{(A13)}$$

Finally, the VRH mean values are obtained by

$$B = \frac{1}{2}(B_V + B_R) \quad \text{(A14)}$$

$$v = \frac{1}{2}(v_V + v_R) \quad \text{(A15)}$$